doi:10.1038/nature11747

SUPPLEMENTARY NOTES

Note S1:
Light offset produced a precise compensatory turn in the direction opposite to the light-evoked turn (Fig. 1g). As a result, the fly's net lateral displacement after this compensatory turn was close to zero (Fig. 1i). A train of light pulses produced a larger turn, and the fly's compensatory turn after light offset was commensurately larger, although less precise (Fig. 1i). This suggests that the fly keeps track of how far it has turned away from its original path, and the accuracy of its estimate depends on how far it has strayed.

Note S2:
Resting GCaMP fluorescence (F) was not significantly different in the right and left glomeruli ($p = 0.67$, $n = 6$, paired t-test). This is expected because each glomerulus contains the axons arising from both the right and left antennae. Although one antenna is removed, the cut axons arising from that antenna are still present in the neuropil. Thus, both right and left glomeruli must contain the same number of GCaMP molecules, and so resting fluorescence is the same. Spontaneous ORN activity evidently makes little contribution to F.

What is the mechanistic basis for the significant ipsi/contra difference in $\Delta F/F$? A previous study reported that an ORN plasma membrane marker is two-fold more abundant in the ipsilateral glomerulus as compared to the contralateral glomerulus[1]. This suggests that the ipsilateral arbor is simply larger than the contralateral arbor of the same ORN. If the properties of ipsi- and contralateral branches are the same, then the ipsi/contra asymmetry in $\Delta F/F$ should be roughly proportional to the ipsi/contra asymmetry in arbor size. In other words, a ~40% difference in $\Delta F/F$ would imply a ~40% difference in the proportion of GCaMP3 signal in each glomerulus arising from the ipsilateral ORN, and thus a ~40% difference in axonal arbor size and neurotransmitter release. (This is smaller than the two-fold ipsi/contra difference in membrane surface area that was described previously[1], but that measurement may include axons of passage, which are found only on the ipsilateral side, and which have a large membrane-to-volume ratio.)

It is unlikely that calcium concentrations are higher in the ipsilateral arbor as compared to the contralateral arbor. Release probability generally depends supralinearly on presynaptic calcium concentration[2] (but see ref 3). Because of this supralinearity, if calcium concentrations were different, we would expect to see an asymmetry in sEPSC amplitude which is considerably larger than the asymmetry in $\Delta F/F$. To the contrary, we observe a roughly equal asymmetry in sEPSC amplitude and $\Delta F/F$, making this scenario less likely.

Note S3:
We found that two arbitrarily-chosen glomeruli (DM1 and DM6) were each sufficient to produce a behavioral turning response when stimulated individually. Moreover, other investigators have found that a variety of odor stimuli produce turning[4-6]. Even aversive stimuli such a benzaldehyde[4] or optogenetic activation of the CO_2-selective ORNs (data not shown) lead to positive osmotropotaxis. Thus, steering is unlikely to be based on the activity of just one or a few glomeruli. Rather, the fly appears to steer based on the pooled activity of most or all glomeruli. Thus, the relevant comparison is between the pooled activity of the entire left antennal lobe, versus the entire right antennal lobe. We saw robust turning in response to an optogenetic stimulus that produced 3 or 4 unilateral spikes in a single ORN type (Figure 1e-j). There are 45 neurons of this type on the antenna[7], amounting to ~150 spikes in the 50-ms stimulus period. *Drosophila* ORNs fire on average ~ 8 spikes/s in the absence of an odor[7,8]. Because there are ~1200 ORNs per antenna[9], this means ~480 spikes per antenna per 50-ms period. Recall that both antennae were intact in the optogenetic experiments, and that ipsilateral synapses are ~40% stronger than contralateral synapses. Thus, the ipsi:contra ratio of incoming input was approximately (1.4×(150+480)+480) divided by ((150+480)+480×1.4), or 1.05. In other words, there was a ~5% difference between the right and left sides of the brain in the level of incoming peripheral input during this 50-ms period.

SUPPLEMENTARY METHODS

Spherical treadmill

The spherical treadmill apparatus was constructed by placing an optical mouse underneath a ¼" hollow HDPE sphere (Precision Plastic Ball Co. LTD, Addingham, Ilkley, UK, and Craigs Technologies, Seaford, DE) (Supplementary Fig. 1a). The plenum of the apparatus was fabricated from a ¼" thick sheet of cell-cast acrylic, and was custom-machined with a ball-nose end mill to be just slightly larger than the floating sphere. While floating, approximately half of the sphere was positioned below the plane of the plenum. We found that the properties of the sphere were critical to the proper functioning of the treadmill. We first sorted 1,611 spheres by weight to identify the lightest ones in the batch. Approximately 100 spheres had a mass equal to or below 80 mg. We next placed each of these lighter spheres in our apparatus to determine which ones had the most spherically uniform weight distribution. Approximately 20 spheres were adequately symmetric. The sphere we selected for this study had a weight of 75 mg and was among the most spherically uniform, as assessed by the duration of its spin after being puffed with a transient jet of air while in the apparatus. This sphere was levitated above the mouse sensor with a jet of air generated from a compressed air cylinder and needle valve (flow rate 250 mL/min).

The electronics were removed from a G9 Laser Gaming Mouse (Logitech, Newark, CA) and positioned beneath the sphere. This mouse and sensor were selected for their high reporting rate (500 Hz at maximum spatial resolution) and the ability to disable sleep mode. We used the sensor to sample the forward and lateral velocity of the sphere; note that we did not measure rotation about the *z*-axis of the sphere (yaw). Data from the optical mouse was imported via USB into Windows XP (Microsoft, Redmond, WA) and extracted using the DirectX command. This allows mouse position values to be calculated before Windows alters their acceleration properties and bounds their limits to the computer's monitor. The position values were acquired in MATLAB (Mathworks, Natick, MA) at 3-4 kHz. The raw mouse positions were converted from pixel values to centimeters by a fixed conversion factor. This factor was calculated by rotating a sphere above the optical sensor and converting the distance traveled on the surface of the sphere from pixels to centimeters. During this calibration, the rotation of the sphere was confined to a single axis by inserting an insect pin through the sphere and inserting the ends of the pin into the narrow ends of two pipette tips to allow rotation along only one axis. After position values were converted from pixels to centimeters, they were filtered in MATLAB using a 2nd order low-pass Butterworth filter with a cut off frequency of 100 Hz, and they were then interpolated at 1 kHz.

Flies used for behavioral experiments were collected from culture bottles one day before the experiment. In order to prevent the head from moving relative to the body, the posterior edge of each eye was glued to the thorax with UV-curable adhesive (KOA 300, Kemxert, York, PA). Flies were then stored in a vial containing a moistened Kimwipe (New Milford, CT) but no food overnight. Just before being placed in the apparatus, flies were cold-anesthetized, glued to a tether consisting of a 200 μm tungsten wire, and positioned onto the treadmill with the guidance of three small video cameras (Fire-i camera, 1394Store, San Ramon, CA) equipped with magnifying lenses to ensure proper alignment. The treadmill was enclosed in a darkened box insulated with sound-absorbing foam. The flies were typically allowed 30-60 min to acclimate to the treadmill before data was acquired. All trials in which the fly's average speed fell below 0.1 cm/s were excluded from our analysis. The percentage of trials excluded was always low (mean % excluded trials per fly, peach odor = 0, pentanoic acid = 3.25 ± 2.9, *Or42b-Gal4*:UAS-ChR = 12.9 ± 4.3, *Orco-Gal4:UAS-ChR* = 21.0 ± 5.6 , *UAS-ChR* controls = 7.5 ± 2.6). To further assess the quality of our behavioral data for each fly, we calculated histograms of the forward velocity (Supplementary Fig. 1c) and lateral velocity (Supplementary Fig. 1e). In our pilot studies, we observed that our best runners displayed a clearly bimodal distribution in their forward running velocity, with a narrow peak centered at zero and a broader but still relatively tight peak centered at approximately 1.5 cm/s. These statistics generally mimic the behavior of free-walking flies[10]. Flies that struggled to turn the sphere produced a histogram where the peak at zero was relatively large, and where the second peak was relatively broad or indistinct. We excluded flies having this type of histogram from our study, prior to any analysis of their turning behavior. We excluded only a minority of flies under each experimental condition, with the only exception to this being the *Orco*^{2} mutants. These flies were poor runners and so over half were excluded from our data set.

Exclusion was determined based purely on the shape of the histogram of forward velocities, but nevertheless this means that behavioral data from this genotype should be interpreted with caution.

Peak lateral velocity was computed as the mean velocity during a time window 500 ms long (for odor experiments) or 50 ms long (for ChR experiments). The window was selected to cover the time when the behavioral response was maximal – i.e., when right and left trials were maximally different. This time window was selected based on the grand average behavior of all flies for a given stimulus condition, and the same window was used in analyzing all flies in that stimulus condition. It was necessary to tailor the analysis window to each stimulus condition because different stimuli produced behavioral responses with slightly different latencies. The window always began at a time point 1.75 - 2.05 s after the air flow began (for odor experiments) or 94 or 95 ms after light onset (for ChR experiments). For the control stimuli, there was no systematic difference between left and right trials, and so the window was placed in the same time point as was used for the peach odor trials. In Figure 1j, the threshold for the onset of the turn was defined individually for each fly. For each fly, we extracted 25 snippets (each 200 ms in duration) from the pre-stimulus period of the trial-averaged velocity trace, and we set the threshold such that <5% of the snippets had a threshold crossing. To find the latency to light-evoked turning behavior for that fly, we then searched a 200 ms period after stimulus onset for the first threshold crossing.

Odor delivery

The behavioral experiments used either peach odor (obtained by filling the odor vial with fermented mashed peach, diluted 10-fold in water) or else pentanoic acid (diluted in water). The olfactometer used for behavioral experiments is schematized in Supplementary Fig. 5a. The olfactometer consisted of two paths, each of which terminated in a thin-walled quartz glass capillary, 700 μm inner diameter (Supplementary Fig. 1a). Airflow through each path was controlled via a syringe pump (NE-510, New Era Pump Systems, Inc. Farmingdale, NY). Air flow into and out of the syringes was controlled by 3-way solenoid valves (Cole Parmer, Vernon Hills, IL). The air from the syringe pumps was directed to either an odor vial or water vial using pinch valves (Clark Solutions, Hudson, MA).

In pilot experiments, we found that flies are sensitive to the clicking of the valves, and their behavior can also depend on the static state of the solenoid valves (which have two positions, activated and deactivated, corresponding to the two outlet streams). Therefore, we designed the olfactometer so that, during the data acquisition period of each trial, air only passes to the fly though deactivated solenoid valves on both the left and right sides, and all the pinch valves and all the solenoid valves are motionless.

Prior to each trial, both solenoid valves were switched to their activated state, and the pumps drew the syringes backward to fill them with carbon-filtered air. Next, both solenoid valves were switched to their deactivated state, and one pinch valve was closed on each side of the apparatus (Supplementary Fig. 5a). Data acquisition began 5 s later. Data acquisition began with a 5 s baseline period. Then, the pumps pushed the syringes forward to push air toward the fly at a nominal rate of 8 mL/min for 15 s. The air flow rate at the fly did not instantaneously reach its maximum value; rather, pressure built up gradually until a steady air flow rate was achieved (after approximately 1 s). Flies tended to make a transient turn to the right as the air flow rate increased during the pressure buildup (open arrowhead in Fig. 1c), suggesting an inherent handedness in the flies, an asymmetry in the positioning of the flies on the ball, or an asymmetry in the functioning of the olfactometer. In any event, the cue for this transient turn must be mechanical rather than olfactory because it was the same regardless of the odor stimulus. In control experiments where the odor vials were replaced with water vials, the fly made the same transient turn to the right, but there was no asymmetry in the fly's behavior during the period when asymmetric odor stimuli caused turning (Supplementary Fig. 5b-c, compare with Fig. 1c-d). This demonstrates that the turning which we interpret as an olfactory behavior must be caused by the odor stimulus. During this 15-s epoch of each trial, each of the two air streams was either odorized or not, depending on the state of the pinch valves (Supplementary Fig. 5a). Then, 15 s after the syringe pumps were turned on, both the left and right air streams were directed to the water vials by the pinch valves, and the air flow rate was increased to 10 mL/min for 5 s in order to flush any odor out the system. Finally, the solenoid valves were switched to their activated state to allow the syringes to reverse direction and draw clean air

through a carbon filter in preparation for the next trial. The activation of the syringe pumps caused a transient electrical artifact in the readout of the spherical treadmill apparatus, and we clipped this artifact from the traces displayed in the Figures. The order of the stimulus conditions was randomized, and each fly was presented with 15 trials of each condition with a 60 second inter-trial interval.

Note that the stimulus is nominally constant throughout the 15-s odor presentation period. Nevertheless, the flies stop turning after several seconds. This may be due in part to adaptation in sensory neurons[8]. The odor stimulus may also decline over the stimulus period.

The olfactometer design used in our electrophysiological recordings has been previously described[1]. Briefly, an air stream (2.2L/min) was passed through activated carbon and directed at the fly through a carrier tube 3 mm in diameter and positioned 8 mm from the fly. Ten percent of this airstream was redirected into the headspace of a vial containing an odor (either pentanoic acid dissolved in water or ethyl acetate dissolved in paraffin oil), and redirected back into the carrier tube. Odor dilutions noted in the text refer to the dilution factor of the odor in the liquid solvent. Odor pulses were 500 ms in duration with an inter-pulse interval of 45 seconds. Typically, flies received 4-6 trials of each odor and these responses were averaged within an experiment.

The use of different olfactometers in behavioral and electrophysiology experiments was necessitated by the different obstructions to air flow on the two experimental setups. In the behavioral experiments, there was no physical obstruction in the vicinity of the fly's head, and so we could create fairly laminar flow of air over the head which prevented excessive mixing of the two air streams. By contrast, on the electrophysiology rig, the head is by necessity surrounded by a flat platform (Supplementary Fig. 3a). This evidently creates turbulence which causes the air streams to mix. As a result, when we delivered odor stimuli that were nominally completely lateralized, we still detected large amounts of odor on the nominally clean side of the fly head. Removing one antennae allowed us to lateralize the odor stimulus in spite of turbulent mixing.

Optogenetic stimulation

Prior to the experiment, the eyes and ocelli of the fly were painted black with waterproof India ink, and UV-curable adhesive was applied over the paint to prevent it from flaking off. The antennae of the fly were immobilized by gluing the second antennal segment to the head capsule of the fly. The distal tips of the funiculus were pointed away from the head, with the long axis of the antenna in the horizontal plane. The optogenetic stimulus consisted of a blue light (475 nm) emitted by a Cree XR-E LED (LED Supply, Randolph, VT) mounted to a heat sink and butt-coupled to a fiber optic filament with a core diameter of 50 μm (AFS50/125Y, Thorlabs, Newton, NJ). The fiber optic filaments were placed immediately lateral to each antenna, and were pointed medially, meaning that the light was not directed into the head capsule (Supplementary Fig. 2).

To confirm that the light stimulation was specific, we systematically recorded from both DM1 ORNs and non-DM1 ORNs. DM1 ORNs were identified based on the size and location of the sensillum, together with the spike waveforms of the ORNs in the sensillum. Light responses we always observed in DM1 ORNs, and were never observed in non-DM1 ORNs. This is consistent with the published work validating the specificity of the Gal4 driver we used to drive ChR expression[11].

In some behavioral experiments with optogenetic stimuli, we strictly alternated between left and right illumination trials. Post hoc, we noticed that this appeared to entrain the flies' walking rhythms across trials; this effect can be seen as an anti-correlation between left and right trials in the baseline period in Fig. 1g. When we began to perform experiments with randomized stimuli, this effect disappeared.

We also noted that the behavioral response triggered by the optogenetic stimulus has a faster onset and a faster offset, as compared to the behavioral response trigged by odor. This may be the result of somewhat greater stimulus-evoked synchrony among ORNs in response to light as compared to odor.

Analysis of spontaneous EPSCs

All sEPSC analysis was performed by an experimenter who was blinded to which PN was ipsi- or contralateral to the intact antenna, and all measured sEPSC event times and amplitudes were verified by visual inspection of each trace. We first subtracted the mean holding current from each trace and detected sEPSCs by smoothing the trace, searching for a local minimum, and counting a sEPSC associated with this minimum if the current

crossed a threshold. Next, we fit the decay phase of each sEPSC with a single exponential and subtracted it from the rest of the trace. The amplitude of each sEPSC was calculated once the contribution of all preceding sEPSCs had been subtracted. In some cases, two events occurred in rapid succession, and so not enough data was available to accurately fit the truncated sEPSC. In this situation, we used the time constant derived from the fit of well-isolated events to model the truncated sEPSC. Periods of a recording in which spontaneous activity was too high to resolve individual sEPSCs were excluded from the analysis. Paired ipsi- and contralateral events were initially assigned to each other according to the order in which they were detected by the algorithm, moving forward in time from the beginning of the trial. *Post hoc*, any events that had a latency greater than 2.5 ms relative to their partner were automatically assigned a new partner by finding a local minimum in the current recorded from the other PN within a window ± 2.5 ms around the event. Visual inspection of the traces showed that this realigned the sEPSC pairings and corrected for small EPSCs that crossed threshold in one PN and not the other. "Unpaired" sEPSCs corresponded to situations where the local minimum detected by the algorithm was rejected by the experimenter because it did not resemble a sEPSC. We recorded an average of 994 sEPSCs from each cell. The latency difference between ipsi- and contralateral EPSCs in this study (0.80±0.51 ms) was larger than that reported previously (0.3±0.10 ms)[12], but the difference does not affect our conclusions in this study; the discrepancy is likely due to differences in the position of the glomeruli where these PN dendrites reside, together with differences in the algorithm used to detect sEPSCs.

Synaptobrevin imaging

We expressed a n-synaptobrevin:GFP fusion protein specifically in DM6 ORNs using the Gal4-UAS system. We used flies heterozygous for both *UAS-n-syb:eGFP* and *Or67d-Gal4*, which drives expression exclusively in DM6 ORNs[13]. One antenna was removed within several days of eclosion. Three days later, after the cut ORN axons had degenerated[1], the brains were removed from the head and fixed in 4% formaldehyde. Primary antibody incubation consisted of 1:50 chicken anti-GFP (Invitrogen) and 1:50 mouse anti-bruchpilot (nc82, Developmental Studies Hybridoma Bank). Secondary incubation consisted of 1:250 anti-chicken:Alexa488 and 1:250 anti-mouse:Alexa633 (Invitrogen). The n-synaptobrevin:eGFP fusion protein localizes selectively to presynaptic neurotransmitter release sites at central synapses[14]. Consistent with this, we observed intense GFP signal in antennal lobe glomeruli (where ORNs release neurotransmitter) and much dimmer signal in ORN axons in the antennal nerve and in the midline commisure. We quantified n-synaptobrevin:GFP fusion protein by measuring total fluoresence in the DM6 glomeruli using the Measure Stack plugin in ImageJ (http://rsbweb.nih.gov/ij/). We drew the boundaries of the glomerulus to exclude the axons of passage wrapping around the border of the ipsilateral glomerulus; this should minimize the contribution of the dim signal in these axons that is unrelated to neurotransmitter release sites.

REFERENCES FOR SUPPLEMENTARY TEXT:

1 Berdnik, D., Chihara, T., Couto, A. & Luo, L. Wiring stability of the adult Drosophila olfactory circuit after lesion. *J. Neurosci.* **26**, 3367-3376, (2006).

2 Dodge, F. A., Jr. & Rahamimoff, R. Co-operative action a calcium ions in transmitter release at the neuromuscular junction. *J Physiol* **193**, 419-432, (1967).

3 Murphy, G. J., Glickfeld, L. L., Balsen, Z. & Isaacson, J. S. Sensory neuron signaling to the brain: properties of transmitter release from olfactory nerve terminals. *J. Neurosci.* **24**, 3023-3030, (2004).

4 Borst, A. & Heisenberg, M. Osmotropotaxis in Drosophila melanogaster. *J. Comp. Physiol. [A]*. **147**, 479-484, (1982).

5 Duistermars, B. J., Chow, D. M. & Frye, M. A. Flies require bilateral sensory input to track odor gradients in flight. *Curr. Biol.* **19**, 1301-1307, (2009).

6 Flugge, C. Geruchliche Raumorientierung von *Drosophila melanogaster*. *Z. Vergl. Phys.* **20**, 463-500, (1934).

7 de Bruyne, M., Foster, K. & Carlson, J. R. Odor coding in the Drosophila antenna. *Neuron* **30**, 537-552, (2001).

8 de Bruyne, M., Clyne, P. J. & Carlson, J. R. Odor coding in a model olfactory organ: the Drosophila maxillary palp. *J. Neurosci.* **19**, 4520-4532, (1999).

9 Stocker, R. F., Lienhard, M. C., Borst, A. & Fischbach, K. F. Neuronal architecture of the antennal lobe in Drosophila melanogaster. *Cell Tissue Res.* **262**, 9-34, (1990).

10 Strauss, R. & Heisenberg, M. Coordination of legs during straight walking and turning in Drosophila melanogaster. *J Comp Physiol A* **167**, 403-412, (1990).

11 Fishilevich, E. & Vosshall, L. B. Genetic and functional subdivision of the Drosophila antennal lobe. *Curr. Biol.* **15**, 1548-1553, (2005).

12 Kazama, H. & Wilson, R. I. Origins of correlated activity in an olfactory circuit. *Nat. Neurosci.* **12**, 1136-1144, (2009).

13 Couto, A., Alenius, M. & Dickson, B. J. Molecular, anatomical, and functional organization of the Drosophila olfactory system. *Curr. Biol.* **15**, 1535-1547, (2005).

14 Kolodziejczyk, A., Sun, X., Meinertzhagen, I. A. & Nassel, D. R. Glutamate, GABA and acetylcholine signaling components in the lamina of the Drosophila visual system. *PLoS One* **3**, e2110, (2008).

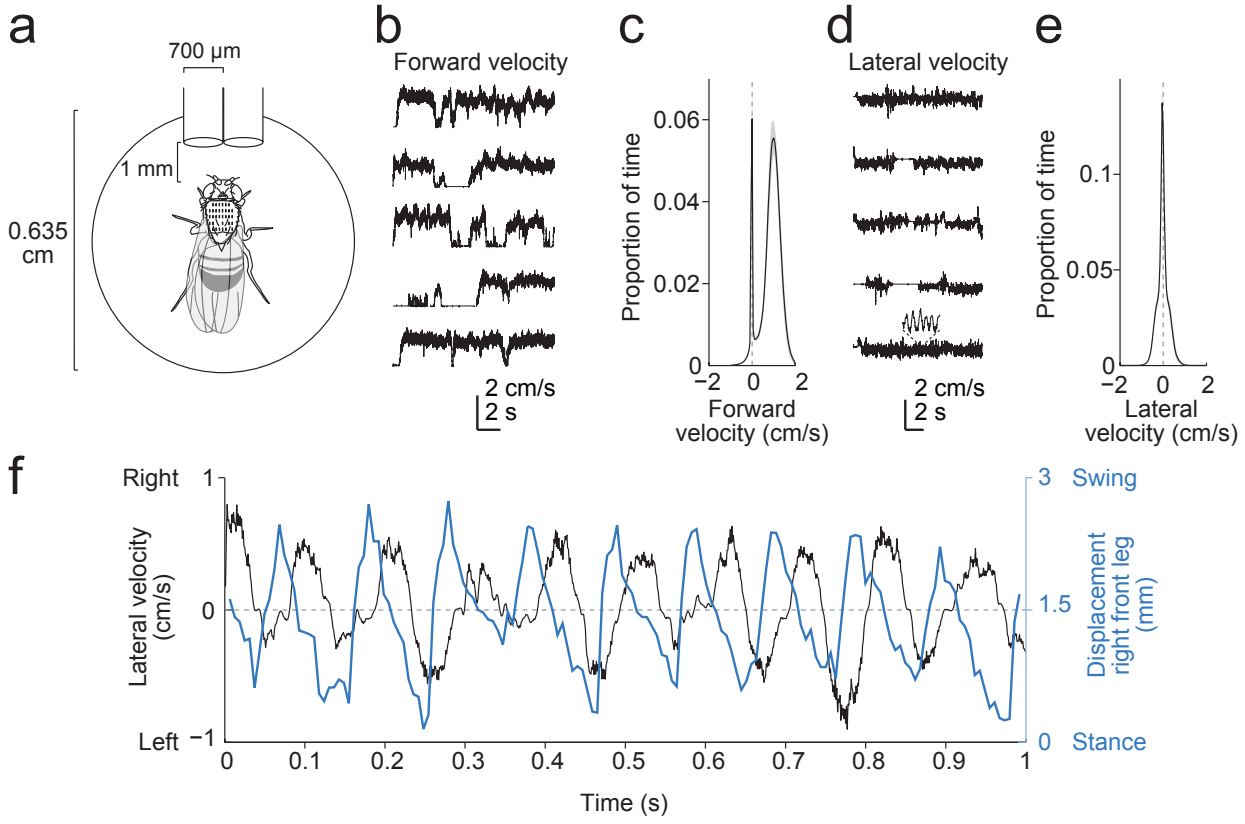

Supplementary Figure 1. Treadmill design and signal interpretation. a, Schematic markers showing critical dimensions of spherical treadmill. During positioning the fly was imaged using microscopic video cameras positioned above, below, and beside the fly to ensure reliable positioning. Fiducial markers were superimposed on each video image and flies were aligned to these markers. **b**, Single-trial recordings of forward velocity versus time show that the fly alternates between bouts of quiescence and episodes of fast running. **c**, A histogram of the proportion of time flies spent running at each forward velocity on the treadmill (n = 8). Flies spent the majority of their time either completely at rest or running approximately 1.5 cm/s. This robust bimodal distribution was used a criterion to include or exclude flies from analysis. All included flies displayed two clear peaks. **d**, Single-trial recordings of lateral velocity versus time, corresponding in time to the traces shown in b. Inset in bottom trace shows oscillations in the fly's lateral velocity. **e**, The distribution of lateral velocities for the same 8 flies shown in c. The lateral velocity typically had a mean of 0 but could deviate slightly if tethering or positioning of the fly on the treadmill was not optimal. **f**, Simultaneous recording of lateral velocity (black) and front right leg position (blue). Leg position was imaged at 160 fps and tracked manually in Matlab. Swing is extension away from the body, while stance is contraction toward the body. As the front right leg begins to contract, the lateral velocity switches from leftward to rightward. The correspondence between lateral velocity and leg position shows that the oscillations in lateral velocity are due to the stride rhythm of the fly. Notice that the stride period is approximately 100 ms, which is the period observed in freely walking flies (Strauss and Heisenberg, 1990).

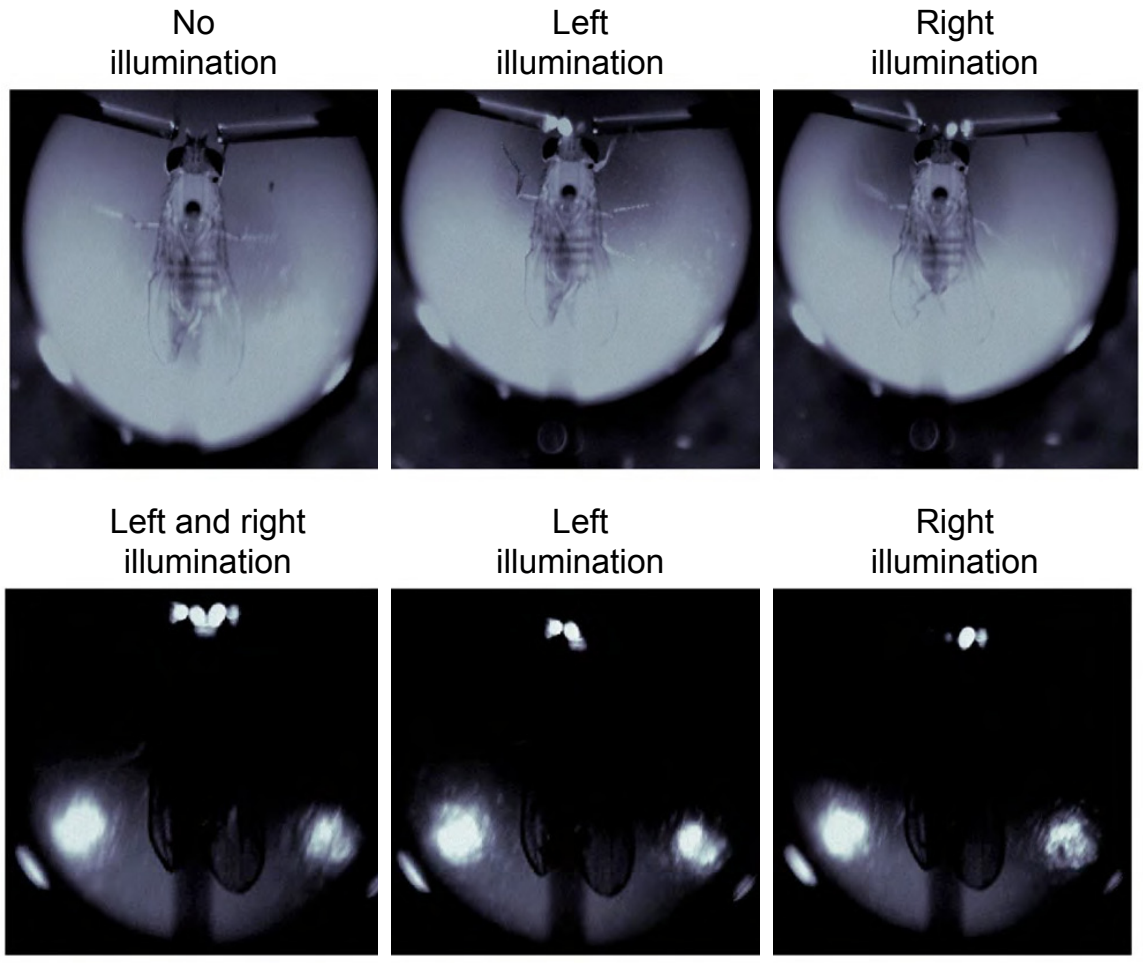

Supplementary Figure 2. Illumination of the fly antenna by fiber optic filaments.
The tethered fly is shown standing on the spherical treadmill, with a fiber optic filament positioned lateral to each antenna. The second antennal segments were glued to the head capsule of the fly, and the antennae were raised so that the distal tips of the funiculus were pointed away from the head, with the long axis of the antenna in the horizontal plane. The fiber optic filaments had a core diameter approximately equal to the dimensions of the funiculus (50 μm). When the LED coupled to the filament was turned on, the entire antenna was illuminated. The filaments were placed immediately lateral to each antenna, and were pointed medially. As a result, the light was not directed into the head capsule. Prior to each behavioral experiment, the eyes and ocelli of the fly were painted black with waterproof India ink, and UV-curable adhesive was applied over the paint to prevent it from flaking off. (Note: in these images, the ocelli are not painted.)

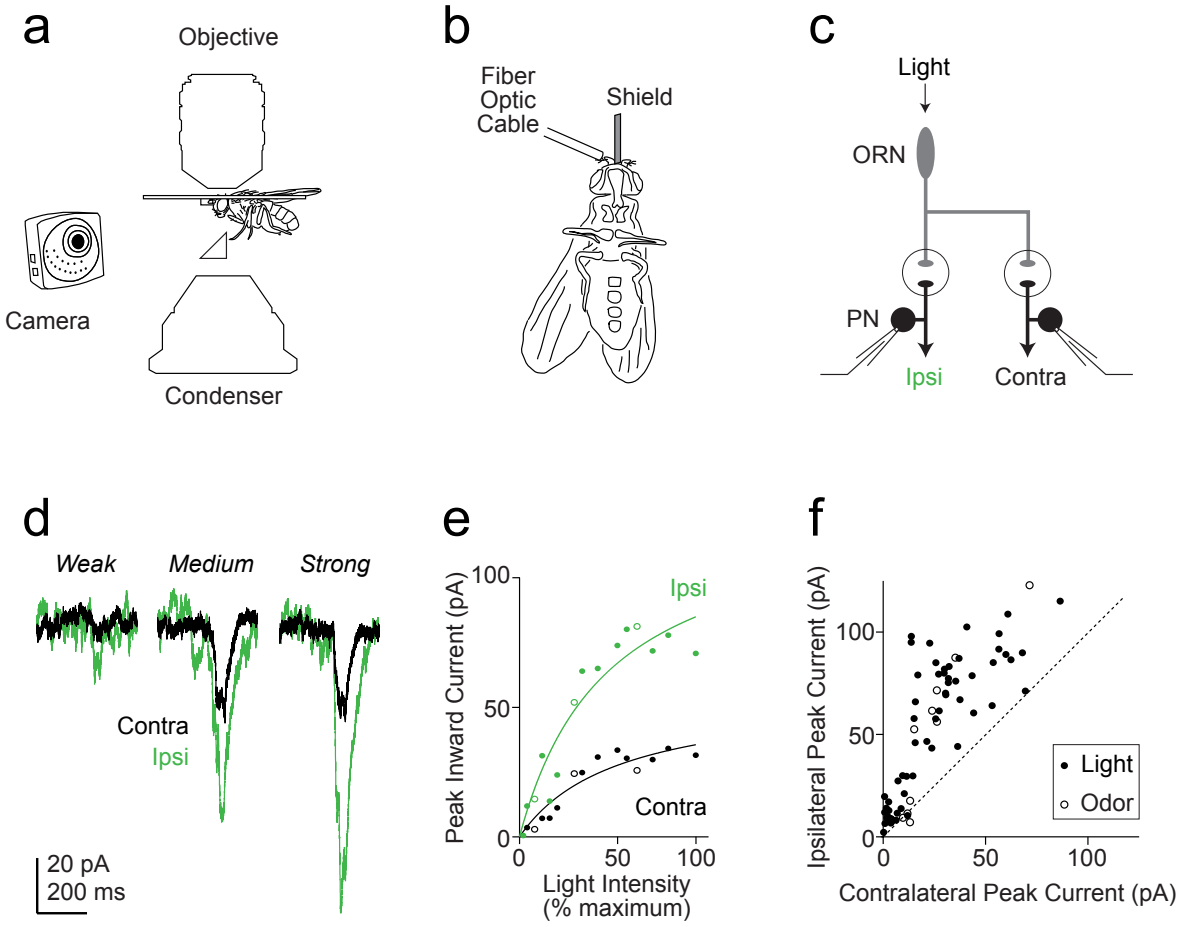

Supplementary Figure 3. Lateralized ORN activity produces an ipsilateral bias in PN synaptic currents. a, Schematic showing optogenetic preparation from the side including mirror (right triangle), microscope equipment, and fly. A camera positioned in front of the fly was used to visualize the fly from either the front or (by focusing on the mirror) from underneath. **b**, The same preparation shown from underneath. A fiber optic cable is positioned next to one antenna, and a foil shield is positioned between the two antennae to block light from reaching the contralateral side. Both antennae are intact. **c**, Schematic showing the recording configuration. One antenna was stimulated with light, while ipsi- and contralateral sister PNs were recorded sequentially in the same preparation. Recordings were performed in whole-cell voltage clamp mode (V_{hold} = -60 mV). The genotype of the flies was *NP3062-Gal4,UAS-CD8:GFP/+;Orco-Gal4/+;UAS-ChR2/+*. **d**, Synaptic currents recorded from a pair of DL5 PNs using low, medium, and strong light intensities to stimulate ipsilateral ORNs. The strongest light intensity corresponds to the strength of light used in Figure 1 of the main text. **e**, The ipsi/contra ratio in synaptic currents is roughly constant across stimulus intensities. Data shown here are from the same experiment as in panel d (open circles correspond to the traces in d). The peak inward current was defined as the mean current over a 30 ms window around the maximum downward deflection. Each point represents the mean of 3-6 trials. **f**, Group data comparing the magnitude of ipsi- and contralateral synaptic currents evoked by the same stimuli in sister PN pairs. This plot contains data from 5 preparations using optogenetic stimuli and 6 experiments using an odor stimulus (pentanoic acid). In each preparation, multiple stimulus intensities were used (3-6 trials per stimulus per preparation). Recorded PNs were in glomerulus DM6, DL5, or DM4. Note that the ipsi/contra asymmetry is similar in the experiments with the optogenetic stimulus (where both antennae were intact) and in the experiments with the olfactory stimulus (where one antenna was removed to lateralize the odor).

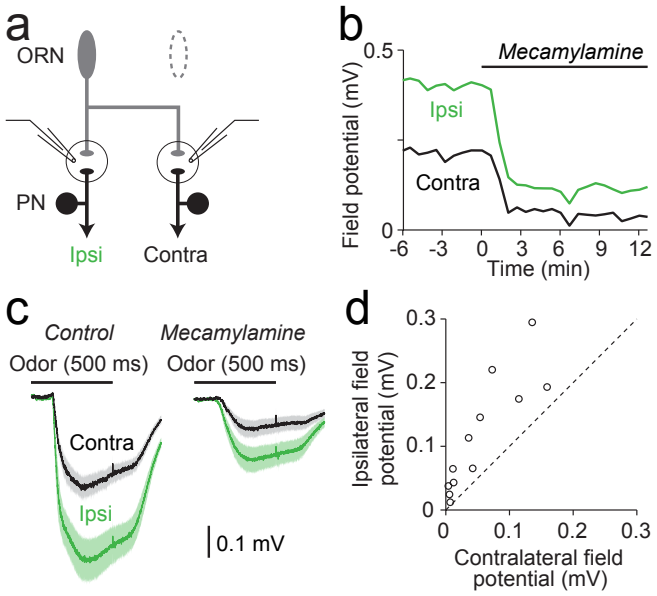

Supplementary Figure 4. Ipsi/contra asymmetry in presynaptic currents. **a**, Schematic of recording configuration. Local field potentials were recorded simultaneously in the right and left DM6 glomeruli. The odor (pentanoic acid) was lateralized by removing one antenna. The local field potential is a measure of the transmembrane currents (both pre- and postsynaptic) in the region of the recording electrode. **b**, A time series of ipsi- and contralateral local field potential amplitudes recorded in a typical experiment. Mecamylamine (200 μM) was added to block nicotinic acetylcholine receptors, thereby isolating the portion of the local field potential associated with the presynaptic side of the synapse. **c**, The odor-evoked field potential (mean ± s.e.m., computed across 8 experiments) is larger in the ipsilateral glomerulus. **d**, Group data for the 8 experiments showing that the ipsi/contra difference (in the presence of mecamylamine) was observed over a range of response magnitudes. Field potential amplitude was measured as the mean over the 500-ms odor stimulus period. The data for each experiment were fit with a line through the origin, and the mean slope of the fitted lines was 3.3 ± 0.9 (slopes were significantly different from unity; $p < 0.01$, Mann-Whitney U test). These data are consistent with the calcium imaging results, and they provide further support for the conclusion that there is an asymmetry in presynaptic activity in ORN axon terminals.

Methods: Saline-filled patch pipettes were inserted into the neuropil of the DM6 glomeruli. These glomeruli was identified as the most dorsal and medial glomeruli identified under GFP fluorescence in *NP3062-Gal4,UAS-CD8:GFP* flies. The odor stimulus was lateralized by removing one antenna. Stimuli were delivered at 45 s intervals. We tested two odor concentrations (10^{-2} and 10^{-3} pentanoic acid) in each of 8 flies, but in 4 of the 8 cases we were not able to measure a bilateral field potential response to the 10^{-3} concentration, and so the data from that concentration was excluded from our analysis for those 4 flies. Each experiment and all subsequent analysis was conducted blind to the identity of which antenna was removed.

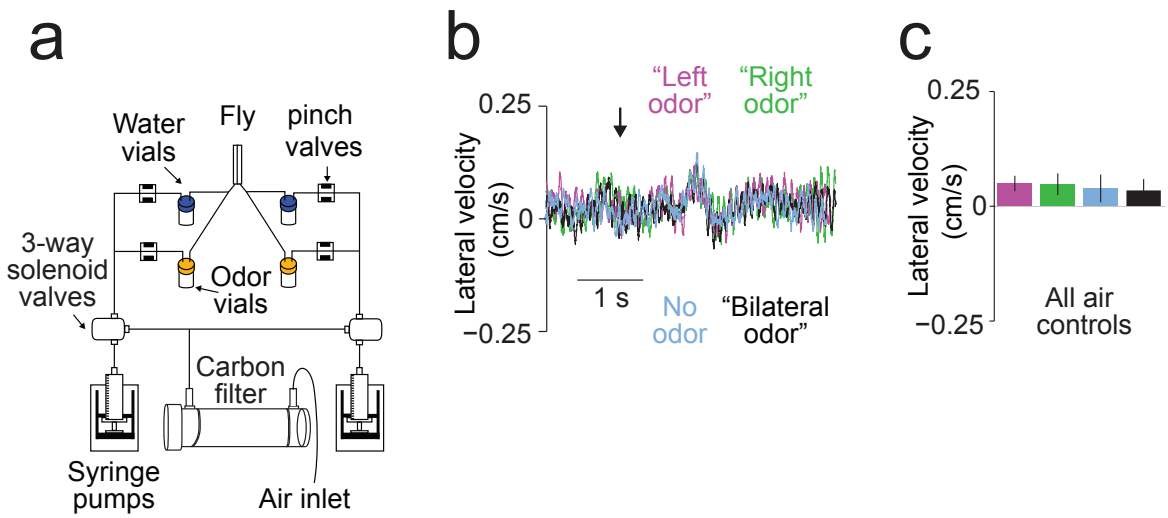

Supplementary Figure 5. Validation and design of olfactometer for behavioral experiments. a, The olfactometer consisted of two paths that started at syringe pumps and led to the head of the fly. Each path could be directed through the headspace of either a vial containing odor (diluted in water), or a vial containing water. Details on the design of the olfactometer are provided in Supplementary Methods. **b**, The mean lateral velocity traces of 7 flies when all four vials contained water only. The labels refer to the nominal olfactometer path, not the actual stimulus. Arrow indicates activation of the syringe pump. Note the small rightward (positive) bias before pump activation, and a small tendency to turn right after pump activation; this is due to either a small asymmetry in the apparatus, or a consistent asymmetry in the positioning of the fly. **c**, With water in all four vials, no statistical difference was seen in the peak lateral velocity, regardless of the path that air took to reach the fly. This demonstrates that the turning behavior we observe in Figure 1 is due to olfactory stimuli, not auditory or other mechanosensory stimuli.